International Conference on Space Optics—ICSO 2018

Chania, Greece

9–12 October 2018

Edited by Zoran Sodnik, Nikos Karafolas, and Bruno Cugny

All-dielectric prism-grating-prism component realized by direct hydrophilic bonding technology for optical applications in space

Thomas Flügel-Paul

Carolin Rothhardt

Tino Benkenstein

Kevin Grabowski

et al.

International Conference on Space Optics — ICSO 2018, edited by Zoran Sodnik, Nikos Karafolas, Bruno Cugny, Proc. of SPIE Vol. 11180, 1118014 · © 2018 ESA and CNES · CCC code: 0277-786X/18/$18 · doi: 10.1117/12.2535959

All-dielectric Prism-Grating-Prism component realized by direct hydrophilic bonding technology for optical applications in space

Thomas Flügel-Paul*[a], Carolin Rothhardt[a], Tino Benkenstein[a], Kevin Grabowski[a], Stefan Risse[a], Ramona Eberhardt[a], Benedikt Guldimann[b], Uwe D. Zeitner[a]
[a]Fraunhofer Institute for Applied Optics and Precision Engineering, Albert-Einstein-Strasse 7, 07745 Jena, Germany; [b]European Space Agency (ESA), European Space Research and Technology Centre (ESTEC), Postbus 299-2200 AG Noordwijk, The Netherlands

ABSTRACT

Here, we report on the approach of realizing an all-fused-silica PGP disperser (prism + grating + prism) by low temperature direct bonding. A surface relief grating with period 660nm and overall depth of approximately 2000nm is sandwiched between two equal prisms. Direct bonding of glass relies on the formation of covalent bonds between hydrophilic silicon-oxide surfaces. Compared to other joining technologies, like adhesive bonding or optical contacting, the established connection is stiff, shows no outgassing, is highly resistant against chemical and radiative degradation and the established optical interface is intrinsically impedance-matched. In summary, two prototypes were realized, optically characterized and successfully underwent environmental testing. The overall diffraction efficiency of the PGP is larger than 90%.

Keywords: diffraction, GRISM, grating, diffraction grating, imaging spectroscopy, optical bonding, optical contacting.

1. INTRODUCTION

In a number of modern earth observation missions high resolution spectrometers, which observe in certain narrow bandwidths are the core instruments. For example, earth-observing instruments which collect the sunlight reflected by the earth's surface are used for atmospheric gas monitoring like O2, CO2 and CH4. These gases are typically observed within 3 sometimes 4 bands, i.e. NIR (750nm), SWIR-1 (1600nm), SWIR-2 (2000nm) and SWIR-3 (2300nm). Some of the optical design concepts with its high requirements on spectral resolution and swath-width rely on combinations of transmission gratings and prisms to balance between spectral resolution and aberrations like smile and keystone[1,2]. Merging the diffraction grating and prism(s) into a single element one typically speaks about GRISMs (grating + prism) or even PGPs (prism + grating + prism). Doing this helps to reduce the overall number of optical interfaces within the system (to reduce losses and straylight) and it helps to reduce effort in alignment of the overall system. Moreover, the diffraction grating is operated in immersion, such that the spectral resolution capabilities of the dispersing element are enhanced by the refractive index of the immersion/bulk material. One example are silicon-immersed gratings/GRISMs which cannot be used, however, at wavelengths below ~1100nm because the substrate material becomes opaque[3].

Here we present the results of realizing high-dispersive transmission elements for space applications, i.e. PGPs (prism + grating + prism) entirely made of fused silica glass. The realized prototype components are optimized for operation in the NIR spectral band (745nm – 775nm). However, the technology is scalable from the UV up to the short wave infrared (SWIR) with the main limitation being only determined by the transmission window of the substrate material, i.e. fused silica. The PGP consists of a binary surface relief grating with period of 660nm and depth of 2000nm which is sandwiched between two fused-silica prisms. We use a two-step direct bonding process in order to join the primary components, i.e. two prisms and a plane-parallel substrate carrying the diffraction grating.

Directly bonded glass shows important benefits for demanding applications in harsh environments like space. Compared to other joining technologies, which are commonly used for optical components like adhesive bonding or optical contacting, plasma-activated direct bonding shows superior properties. The formed connection is stiff, shows no outgassing and is highly resistant against chemical and radiative degradation. Moreover, the established optical interface is intrinsically impedance-matched such that Fresnel losses are fully suppressed because no additional material is involved.

The paper is organized as follows: In Section 2 we briefly outline the PGP and the grating design. In Section 3 and 4 we report about the grating and bonding manufacturing process. The performance of the PGP prototype with optical measurements will be presented in Section 5. The paper ends with a short conclusion.

*thomas.fluegel-paul@iof.fraunhofer.de; phone +49 3641 807434; www.iof.fraunhofer.de

2. PGP AND GRATING DESIGN

2.1 PGP Design

The fundamental optical concept and the geometrical dimensions of the PGP are depicted in Figure 1. In particular, the projection of the system into the plane of dispersion is shown. The input beam is collimated, has a circular shape with diameter of 58mm and it propagates along the optical axis. The overall configuration is highly symmetric, i.e. both prisms are equilateral with side lengths of 130mm and the inner angles are always 60°, respectively. The depth of the overall element ("into the display") is 60mm. The input beam hits the entrance facet under an angle of incidence (AOI) of 60° and thus its projection yields an elliptical beam with extension of ~117mm x 58mm.

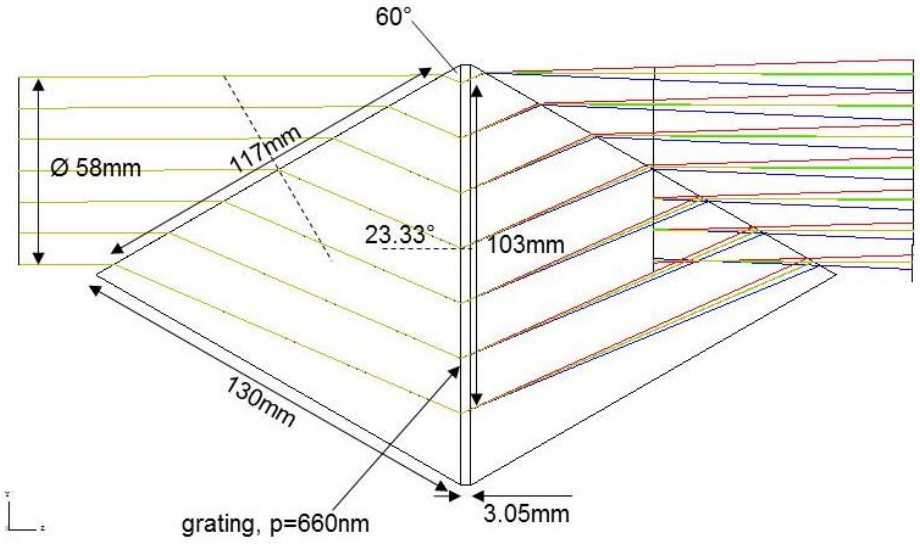

Figure 1. Sketch of the optical beam path through the PGP disperser.

In between both equilateral prisms the diffraction grating is encapsulated on a 3mm thick fused silica substrate. The grating is operated in Littrow configuration, i.e. AOI and angle of diffraction of the central wavelength (760nm) are equal. The same is true for the entire PGP element, meaning that the diffracted beam at Littrow wavelength propagates along the optical axis after leaving the element. This configuration is highly preferred in order to arrange all optical components of the instrument's channel (disperser + imager + detector) on a common and single optical axis.

2.2 Grating Design

The particular grating design is driven by two major specifications. First, the minimum angular resolution of the overall PGP disperser and, second, the required throughput and polarization sensitivity of the PGP device. The first requirement translates into an upper threshold of the gratings period and the latter can only be influenced by the geometry of the grating's nanostructure itself. In the current project, the goal was to design and built a PGO disperser with angular dispersion of >0.15deg/nm and a minimum diffraction efficiency of 90%.

In consequence, the diffraction grating is realized as a surface relief structure which is etched/patterned into a fused silica carrier substrate. A sketch of the structure is provided by Figure 2. It is a binary structure of air voids/grooves which are entirely encapsulated between two fused silica bulk domains on "top and bottom". In the chosen configuration, the calculated diffraction efficiency of the grating lies well above 95%. The polarization sensitivity is smaller than 2% being

determined according to $|I_{TE} - I_{TM}| / |I_{TE} + I_{TM}|$ with $I_{TE/TM}$ being the diffraction efficiencies in TE/TM polarization. In order to reach such good performance in diffraction efficiency and polarization sensitivity the grating is characterized by small and deep air grooves with an aspect ratio larger than 1:8.

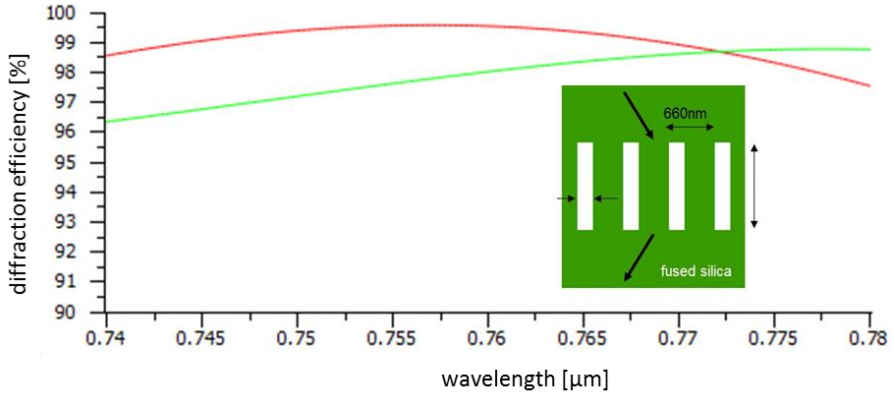

Figure 2. Diffraction efficiency of the ideal binary grating profile. The red (green) curve are the TE (TM) polarization efficiencies. The inset shows the fundamental geometrical layout.

3. GRATING MANUFACTURING PROCESS

The manufacturing process of the PGP element consists of three major steps and goes as follows:

1) Electron beam lithography and deep-reactive ion etching is used to manufacture binary surface relief gratings into a plane-parallel fused silica substrate.
2) The grating is then joined to the first prism by direct bonding and subsequently annealed to establish a first strong bond (PG).
3) The second prism and the PG are finally merged. The entire process flow is performed in cleanroom environment. The planarity of the PG and the second prism are controlled and enhanced in a feedback loop, i.e. interferometric measurements and surface finishing is mutually repeated until the surfaces match to a high precision.

3.1 Grating Manufacturing

We use electron-beam lithography and reactive ion etching (RIE) to realize surface relief structures on bulky substrates[4,5,6]. In the present scenario, the substrate material is fused silica, but it might be also other materials as long as the surface is coated with SiO_2. The main process flow is depicted in Figure 3. The substrate is coated by a metal mask (Cr) which is again coated by an electron sensitive resist. The resist is exposed to electron beam radiation which defines the binary grating pattern. Two subsequent dry RIE-process are used to i) transfer the resist into the metal mask and ii) to transfer the metal mask into the underlying SiO_2 material.

Figure 3. Manufacturing process of binary surface relief gratings by e-beam lithography (left image) and reactive ion etching of the chromium layer (middle image) and SiO2 (right image).

The entire manufacturing process is monitored and controlled by various inspection methods, e.g. SEM and AFM. This allows verifying and eventually correcting for correct feature size and depth level. Figure 4 shows an SEM image in cross-section of the final surface relief structure. The side walls of the grating ridges are not perfectly perpendicular, but the groove width becomes smaller with increasing depth. Most importantly, the top of the ridges is perfectly flat which is guaranteed by the protective functionality of the metal mask during the entire etching process. In particular, the surface roughness is equal to those of the initial substrate such that the bonding process will not be negatively affected (see also Section 3.X).

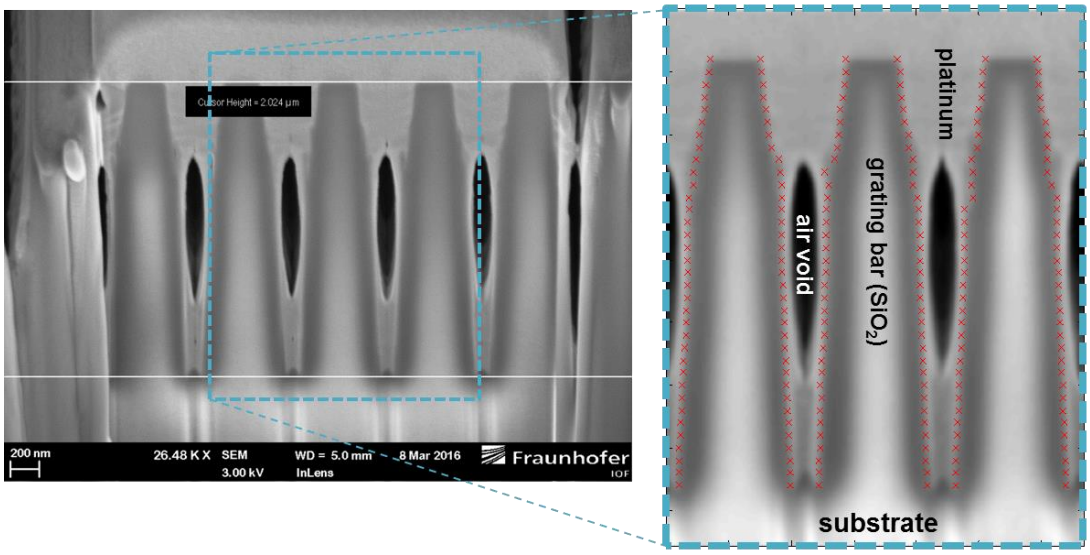

Figure 4. Cross section profile of the grating ridges achieved by focused ion beam milling and SEM inspection. The platinum (Pt) is only deposited for inspection purposes in order to mechanically stabilize the nanostructures during milling process. The air voids are a consequence of the Pt-deposition process and they do not appear in the remaining grating. The red symbols highlight the outer surface of the grating ridges and they are directly extracted from the SEM image.

3.2 Straylight Performance

The stray light performance of the grating was measured via ALBATROSS, an angle-resolved light scattering setup capable of scanning the ARS over the entire hemisphere (in polar and azimuthal direction). Figure 5 shows a typical measurement of the ARS around the signal order (-1st diffraction order in transmission). The scattering background shows a nearly constant profile throughout the entire scanning region between -20° and +20° around the signal order. Most interestingly, the signal peak drops down very rapidly within an interval of only 2° to 3° before it approaches the constant background level of ~10^{-2} sr^{-1} for the detector scanning in the plane of dispersion. When leaving the plane-of dispersion then ARS drops down between 1 and 2 orders of magnitude as also presented in Figure 5 by the red/orange curves.

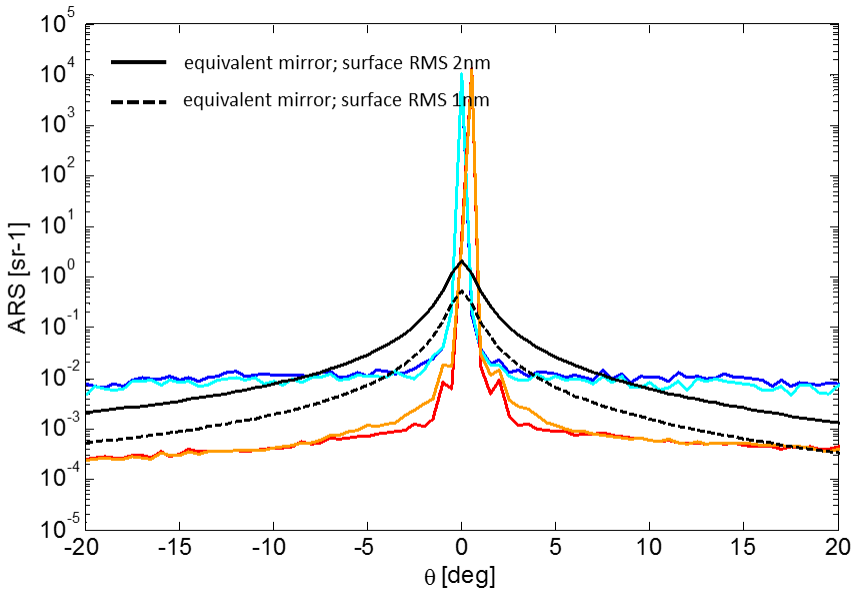

Figure 5. ARS-measurement results of the grating. The curves in blue/cyan (red/orange) are measured in-dispersion plane (45°-out of dispersion plane). The blue/red (cyan/orange) curves correspond to two different measurement positions on the grating surface. The black curves show the ARS of an equivalent plane mirror with RMS roughness 1nm and 2nm, respectively according to Wein's formula[7].

4. BONDING PROCESS

The final PGP element is realized by hydrophilic direct bonding of three components, i.e. the grating substrate and two prisms. The surfaces to be bonded need to be plane and extremely smooth. Although bonding becomes possible at a surface roughness of about 1 nm root-mean-square (RMS), values of <0.3 nm RMS are recommended to obtain high bond strength. For thick and stiff specimen –like prisms– about λ/10 surface flatness peak-to-valley (PV) is required (λ=633 nm), while this prerequisite may be relaxed by more than an order of magnitude for thin and flexible substrates. However, the bonding between the PG component and the (second) counterprism requires a high quality and reliable preparation in order to meet the above parameters.

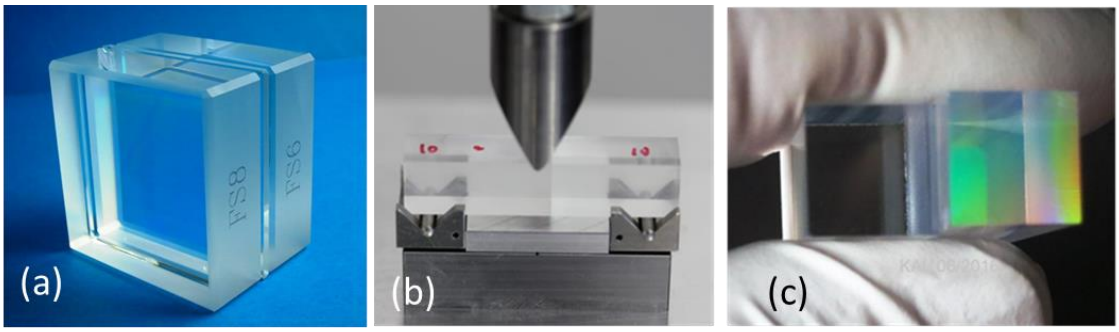

Figure 6. a) Photograph of a bonding test sample used for process development. b) Three-point bending test setup for determining the mechanical strength of the joined component. c) Typical fracture result after bending.

The actual bonding process is performed in clean room environment and it starts with careful cleaning and inspection of particles contamination. The surfaces are then activated by oxygen plasma and afterwards purged by water[8,9]. Contacting of both parts is performed under atmospheric pressure within special mechanical equipment designed and constructed

particularly for this purpose and the individual dimensions of both parts. During the final stages of assembly, the alignment between both specimens (grating substrate + prism) is ensured by mechanical stops. The bonding procedure is completed by a baking process at about 200°C under moderate compressive pressure in vacuum.

4.1 Test Samples and Mechanical Stability.

The final PGP will include two directly bonded interfaces, one between two uncorrugated surfaces and a second where the surface relief structure of the diffraction grating is bonded to a bulky fused silica counterpart. Especially, the interface which involves the surface relief structure will most likely have less mechanical stability (due to reduced contacting area) – a measure which must thus be determined quantitatively.

In order to do so, we have first manufactured small bonding test samples (see Figure 6a) of size 55x55x43mm³. The individual building blocks are two fused silica cuboids of size 55x55x20mm³ and a small test grating substrate of size 55x55x3mm³. One can see the labeling “FS8” or “FS6” on the cuboids’ side faces in Figure 6a. The final bonding test samples were then cut into small bars of size 9.5x9.5x43mm³. A Zwick-Roell testing machine of type Z020 and a 3-point bending test set-up as illustrated in Figure 6b were used and ensembles of 8 specimens were tested. Since the direction of load impact relative to the grating structure was found appreciable, the most sensible orientation (with the grating dispersion direction normal to the load direction) was chosen. Load was applied symmetrically to the middle of both bonding planes and fraction occurred neatly in the grating plane in almost all cases. The bond strength of the uncorrugated interface was measured to be ~1/2 of that of the bulk reference structure (small bulky bars without any bonded interface). The bond strength of the grating interface amounts to only 1/3 of the uncorrugated interface and, in consequence, to ~1/6 in comparison with the bulk reference structure. The factor of 1/3 corresponds nearly to the intrinsical loss in contacting area which is attributed to the encapsulated air voids (grating grooves).

5. PGP PROTOTYPE PERFORMANCE

A photograph of the final full-size prototype PGP is depicted in Figure 7. One can nicely see the elliptical grating area in the inner of the element. Due to technological reasons, the grating substrate overhangs by ~5mm on the left side of the PGP. The remaining side faces are pushed in flush with each other. The maximum alignment error in rotation between the individual components was measured to be 2 arcmin. However, this value is somewhat arbitrary (since no specific requirement exists) and it thus simply determines typical values which can be achieved with standard effort.

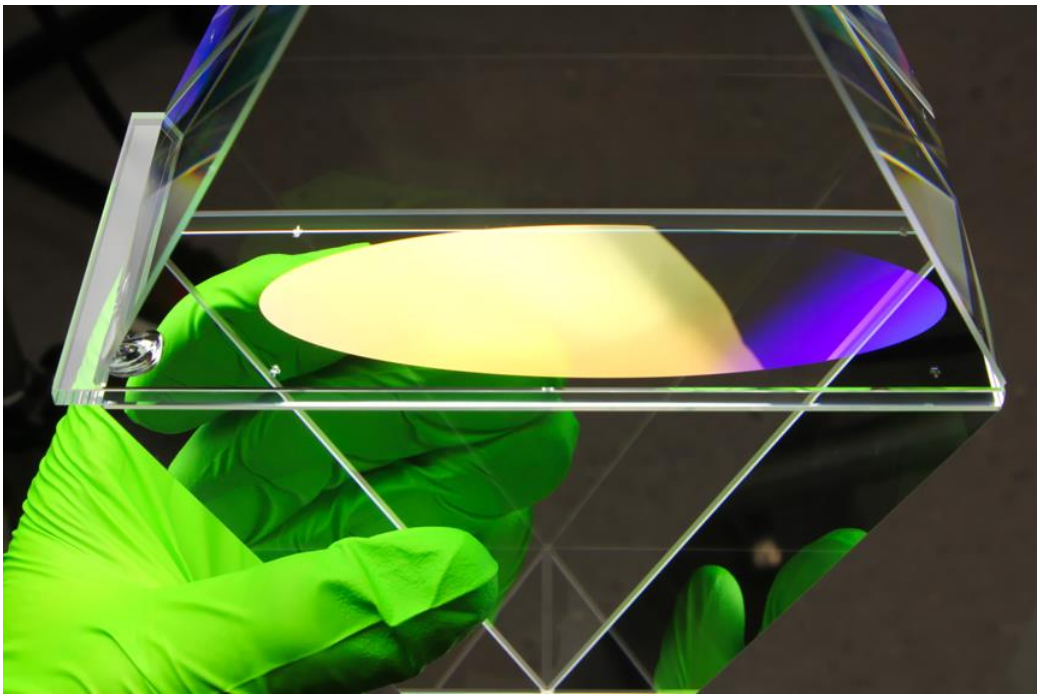

Figure 7. Photograph of the final full-size PGP demonstrator after bonding.

5.1 AR coating and Environmental Testing.

Due to high Fresnel losses of ~$1.0\text{-}0.84^2$ = 30% in TE polarization at the entrance and exit facet of the PGP, an AR coating must be applied in order to achieve overall efficiencies larger than 90%. An interference layer stack between high and low-index dielectrics was used in order to apply an equal AR-coating on entrance and exit facet of the PGP. Two photographs in Figure 8 show the result.

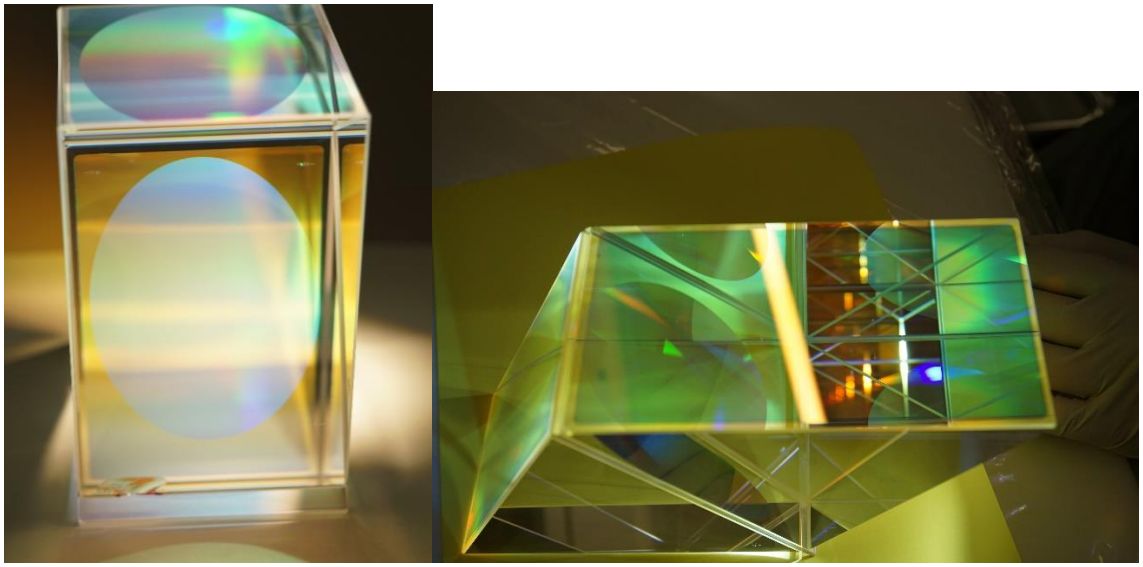

Figure 8. The same PGP demonstrator after AR coating applied to entrance and exit surface of the prisms.AR coating can be identified by the thin circumventing edge in the right photograph where no coating is applied due to mounting issues.

After AR coating, the PGP underwent 8 thermal-vacuum-cycles at temperatures between 0°C and 40°C at pressures down to 10^{-6} mbar. Measurements of the diffraction efficiency as well as visual inspection before and after thermal cycling revealed no degradation of the element and the diffraction efficiency was proven to be unaffected.

Table 1. Measured diffraction efficiency of the PGP at three wavelength. The performance of the double-pass AR coating can be recognized by measurements before and after the coating process. The presented values are the spatial average throughout the clear aperture of the element.

	with AR-coating		before AR-coating (Fresnel losses corrected)	
Wavelength [nm]	**TE [%]**	**TM [%]**	**TE [%]**	**TM [%]**
745	88.6	95.5	91.6	96.7
760	92.0	96.0	93.9	97.2
775	94.9	94.9	95.6	96.1

Table 1 presents the diffraction efficiency of the prototype at three discrete wavelength within the NIR band. The measurement was performed by using a narrow-band and tunable laser source. The efficiency was measured before and after AR coating. At the short wavelength limit, the overall efficiency in TE polarization slightly falls below 90%. However, it is a question of further process optimizations (AR coating and grating manufacturing) in order to come closer to the theoretical limits as provided by Figure 2.

Finally, a second PGP prototype was exposed to gamma radiation of a Co-60 source. After irradiation of 20krad (Si) no visible degradation of the PGP was observed. More importantly, this observation was again verified by a diffraction efficiency measurement (performed 18h after irradiation).

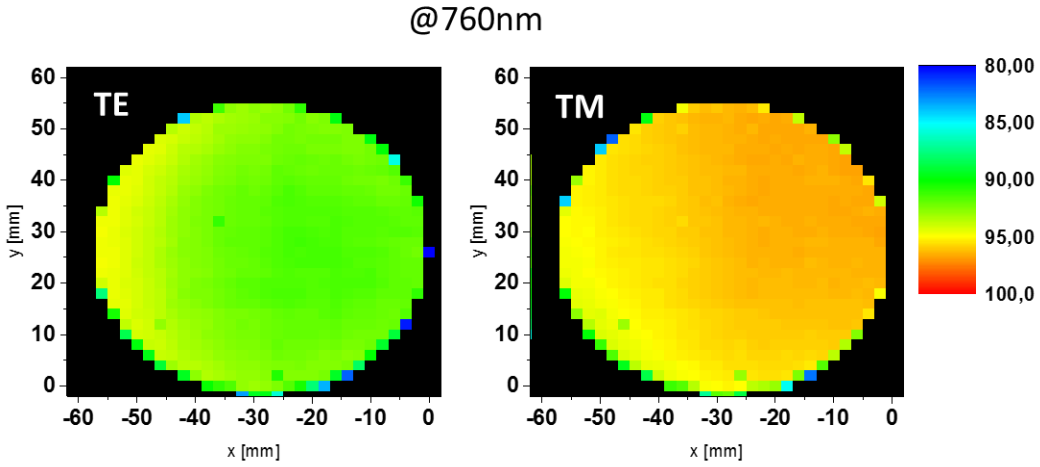

Figure 9. Spatial mapping of the diffraction efficiency over the clear aperture at a wavelength of 760nm.

The data in Table 1 is the spatial average throughout the clear aperture of the PGP. The actual measurement was done with a spot size of ~2mm and an equidistant spatial mapping was performed. Figure 9 shows a representative outcome of such measurement at the center of the NIR band. One can see that the efficiency is nicely uniform throughout the clear aperture with a slight gradient to the edges. However, the performance of a typical imaging spectrometer is mainly driven by the integrated rather the locally resolved efficiency of the main disperser.

6. SUMMARY AND ACKNOWLEDGEMENT

We have applied direct glass-to-glass bonding in order to encapsulate a high performance surface relief diffraction grating between two massive prisms. We succeeded in manufacturing of a large-size prism-grating-prism (PGP) disperser for space instrumentation. The PGP works in transmission and it is entirely made of fused silica glass. It is thus intrinsically impedance matched, which eliminates optical losses. It is also intrinsically thermally matched such that mechanical stresses are minimized and wavefront stability is superior. The optical throughput is between 90% - 95% throughout the entire bandwidth. The potential fields of application span from the deep ultraviolet region (DUV) up to the short-wave infrared (SWIR) with the main limitation determined by transparency of the bulk material.

The work was performed in the frame of the activity "NIR immersed grating in transmission for high resolution spectroscopy" under grant number 4000114780/15/NL/KML funded by the European Space Agency.

We furthermore thank G. Kalkowski and F. Dreisow for their former contribution and valuable discussion.

REFERENCES

[1] Aikio, M., “Hyperspectral prism-grating-prism imaging spectrograph,” VTT, <https://www.vtt.fi/inf/pdf/publications/2001/P435.pdf> (14 August 2018).
[2] Report for mission selection: CarbonSat - An earth explorer to observe greenhouse gases (ESA SP-1330/1), ESA Communications, Noordwijk, The Netherlands, June 2015
[3] Van Amerongen, A., et al., “State of the art in silicon immersed gratings for space,” Proc. SPIE 10564, 05642R (2012)
[4] Zeitner, U.D., Fuchs F., Kley, E.-B., and Tünnermann A., "High-refractive-index gratings for spectroscopic and Laser applications," Proc. SPIE **8995**, 899504 (2014)
[5] Zeitner, U.D., Oliva, M., Fuchs, F., Michaelis, D., Benkenstein, T., Harzendorf, T., and Kley, E.-B., „High performance diffraction gratings made by e-beam lithography,“ Apl. Phys. A 109, 789-796 (2012)
[6] Flügel-Paul, T., Kalkowski, G., Benkenstein, T., Harzendorf, T., Matthes, A., and Zeitner, U. D., „ New grating concepts in the NIR and SWIR spectral band for high resolution earth-observation spectrometers,“ Proc. SPIE 9912, 99122A (2016)

[7] Harnisch B., Deep A., Vink R., and Coatantiec C., "Grating scattering BRDF and imaging performances: A test survey performed in the frame of the flex mission," Proc. SPIE 10564, 105642P (2012)
[8] Kalkowski, G., Harnisch, G., Grabowski, K., Benkenstein, T., Ehrhardt, S., Zeitner, U., and Risse, S., "Low temperature GRISM direct bonding," Proc. SPIE 9574, 95740K-1–K-9 (2015).
[9] Kalkowski, G., Grabowski, K., Harnisch, G., Flügel-Paul, T., Zeitner, U.D., and Risse, S., "Grism manufacturing by low temperature mineral bonding ," Proc. SPIE 10562, 1056204 (2017).